J Wood Sci (2013) 59:104–111
DOI 10.1007/s10086-012-1315-1

ORIGINAL ARTICLE

In situ measurement of tensile elastic moduli of individual component polymers with a 3D assembly mode in wood cell walls

Yasuki Takeichi · Masato Yoshida · Kohei Kitano · Noritsugu Terashima · Hiroyuki Yamamoto

Received: 9 December 2011 / Accepted: 3 December 2012 / Published online: 11 December 2012

Abstract We attempted to measure in situ the tensile elastic moduli of individual component polymers with a three-dimensional (3D) assembly mode in the cell walls of Sugi (*Cryptomeria japonica* D. Don) without isolating the polymers. To prepare wood tangential slices [50 × 6 × 0.2 mm (L × T × R)] consisting of lignin with a 3D assembly mode in the cell walls, cellulose and hemicellulose were removed using the method of Terashima and Yoshida (2006) to obtain methylated periodate lignin slices. To prepare wood slices consisting of polysaccharide with a 3D assembly mode in the cell walls, lignin was removed using the method of Maekawa and Koshijima (1983) to obtain holocellulose slices. Static tensile test was applied to determine the elastic moduli of 3D lignin and 3D polysaccharide slices. The followings were revealed. The elastic modulus of the 3D lignin slices was 2.8 GPa, regardless of the microfibril angle (MFA) in the slices. The elastic moduli of the 3D polysaccharide slices with MFAs of 14°, 23°, 34°, and 42° were 18, 12, 9, and 4 GPa, respectively. The former shows that the lignin with a 3D assembly mode behaves as an isotropic substance in the cell walls, while the latter suggests that the 3D polysaccharide slice shows marked anisotropic structure in the cell wall. Despite the fact that cellulose content increased after lignin removal, values of substantial elastic modulus of the cell wall slightly decreased regardless of MFA. Following two possible reasons were pointed out for explaining this phenomenon. First, lignin removal caused an artifactual deterioration in the polysaccharide slices at the level of macromolecular aggregate. Second, rigid and fusiform-shaped cellulose crystallites are dispersed in the soft matrix of amorphous polysaccharide, and those are loosely connected to each other by the intermediary of matrix polysaccharide. Those suggest that the rigid cellulose crystallite can optimize its strong mechanical performance in the polysaccharide framework of the wood cell wall in combination with the ligninification.

Keywords Lignin removal · Polysaccharide removal · Cellulose microfibrils · Young's modulus

Introduction

The mechanical properties of wood cell walls depend highly on the structural arrangement and properties of the wood polymers within the cell walls, including cellulose, hemicellulose, and lignin. Cell walls are a fiber-reinforced composite system in which cellulose microfibrils act as reinforcement in a lignin-hemicellulose matrix. The intricate 3D intertwining of wood polymers makes wood a strong and flexible material [1, 2]. To better understand the mechanical properties of wood, it is important to investigate the in situ mechanical properties of the individual component polymers in relation to their structure in the cell walls.

In general, cellulose microfibrils are the main contributor to the mechanical properties of wood cell walls because of their highly crystalline structure. The spatial angle between cellulose microfibrils and the longitudinal axis, i.e., the microfibril angle (MFA), of the middle layer

Part of this study was presented at the 61th Annual Meeting of the Japan Wood Research Society in Kyoto, March 2011.

Y. Takeichi · M. Yoshida (✉) · K. Kitano · H. Yamamoto
Graduate School of Bioagricultural Sciences,
Nagoya University, Nagoya 464-8601, Japan
e-mail: yoshida@agr.nagoya-u.ac.jp

N. Terashima
2-610 Uedayama Tenpaku, 468-0001 Nagoya, Japan

of the secondary wall is important in determining the mechanical and physical properties of wood fibers [1, 3–6]. Hemicellulose is a non-crystalline polysaccharide distributed inhomogeneously in cell walls. Hemicellulose is bound to cellulose and lignin by hydrogen and covalent bonds, respectively [7, 8]. Consequently, hemicellulose is essential for maintaining cell wall assembly. Hemicellulose controls cellulose microfibril aggregation and the distance between them [9]. Lignin is an isotropic three-dimensional (3D) macromolecule that forms bead-like modules in the hemicellulose gel that fills the space between cellulose microfibrils [10]. According to Akerholm and Salmen [11], phenylpropane units in lignin are oriented in the direction of the cellulose microfibrils. The same could be true for the matrix polymers of hemicellulose and lignin.

Several studies concerning the elastic properties of isolated wood polymers have been reported. For instance, the elastic longitudinal modulus of cellulose I purified from ramie has been reported as 134 GPa [12, 13]. Cousins [14] reported that the elastic modulus of periodate lignin isolated from *Pinus radiata* is 4 GPa at 10 % moisture content. He also reported that the elastic modulus of the isolated Klason lignin is 3 GPa at 8 % moisture content. However, these values may only be taken as approximations to the in situ polymer properties, because both the molecular structures and the spatial arrangements of these polymers differ substantially in their isolated forms and within the 3D assembly mode in the cell wall. The intricate 3D intertwining of wood polymers influences the mechanical properties of wood cell walls. Therefore, the mechanical properties of the individual polymers must be investigated in situ to determine their influences on the mechanical performance of the wood at the cell wall level.

This study focused on the in situ tensile elastic moduli of the individual component polymers with a 3D assembly mode in the cell walls using the wood specimen with different MFAs. To prepare wood slices consisting of lignin with a 3D assembly mode in the cell walls, cellulose and hemicellulose were removed from Sugi (*Cryptomeria japonica* D. Don) wood slices using the method of Terashima and Yoshida [10] to obtain methylated periodate lignin slices. To prepare wood slices consisting of polysaccharide with a 3D assembly mode in the cell walls, lignin was removed using the method of Maekawa and Koshijima [15] to obtain holocellulose slices. Then, the longitudinal elastic moduli of these slices were measured, and the obtained results were discussed in relation to the elastic moduli of the isolated wood polymers that had been reported by previous authors. We thus aimed to understand how the individual component polymers and their 3D assembly mode optimize the mechanical performance of the wood cell wall.

Materials and methods

Sample preparation

Two 36-year-old Sugi trees (*Cryptomeria japonica* D. Don) in the Nagoya University experimental forest were used. Wood blocks were cut from the trunk at chest height. As mentioned in "Introduction", wood cell wall consists of cellulose microfibrils as the unidirectional reinforcing element and lignin-hemicellulose compound as the compliant matrix. Thus, the mechanical properties of wood cell walls are dependent on the orientation angle of the cellulose microfibrils. To understand the in situ mechanical properties of the individual component polymers, it is useful to measure the relationships between mechanical properties and MFA in wood cell walls. We therefore prepared the wood samples with differing MFAs.

The average MFA in the earlywood region of every annual ring of the wood blocks was measured using an X-ray diffractometer (Shimazu XD-D1w) [16]. Four annual rings with MFAs of 14°, 23°, 34°, and 42° were selected for the study. In total, seventy 50 × 6 × 0.2 mm (L × T × R) tangential slices were sliced from the earlywood region of the individual rings using a sliding microtome.

To prepare the 3D lignin slices, cellulose and hemicellulose were removed from half of the slices using the method of Terashima and Yoshida [10]. The slices were methylated with diazomethane to prevent the modification of the free phenolic hydroxyl group of the guaiacyl unit in lignin. After dehydrating in ethanol, the slices were placed in diethyl ether. Diazomethane was added to the ether and the slices were methylated in the dark for 2 weeks. As the yellow color of diazomethane disappeared during methylation, an equivalent amount of diazomethane was added to the slices. Aqueous sodium periodate solution (2.5 M, pH 3.5, 40 mL) was added to the methylated slices, which were then kept at 50 °C in the dark for 24 h. The slices were washed with water and treated with dilute sulfuric acid at 50 °C in the dark for 24 h, and washed with water. For graded polysaccharide removal, periodate oxidation and hydrolysis were repeated four times. After polysaccharide removal, the slices were held between two glass slides to prevent warping during drying at room temperature.

To prepare the 3D polysaccharide slices, lignin was removed from the remaining slices using the method of Maekawa and Koshijima [15]. Sodium chlorite (1 g) and acetate buffer (0.2 M, pH 3.5, 30 mL) were added to the slices, which were kept at 75 °C. For graded lignin removal, sodium chlorite and acetate buffer were added six times over 1 h. After lignin removal, the slices were dehydrated in a series of graded water–ethanol solutions and then freeze–dried with *t*-butanol.

Wood polysaccharide and lignin removal estimations

To estimate the degree of polysaccharide removal, the oven-dried weight and relative crystallinity were measured after each treatment step. A total of 0.28 g of untreated slices was weighed. An electronic balance with an accuracy of 0.1 mg was used. To measure the crystallinity, slice diffraction patterns were obtained in a 2θ angular range from 5 to 40° using an X-ray diffractometer. The degree of relative crystallinity was calculated from the diffraction patterns using the method of Alexander [17].

To estimate the degree of lignin removal, the oven-dried weight and ultraviolet (UV) absorbance were measured after each treatment step. A total of 0.84 g of untreated slices was weighed. For UV absorbance, the slices were embedded in epoxy resin. Cross-sections 1 μm thick were cut with a glass knife and mounted on quartz slides with glycerin. The sections were observed at wavelengths of 270–280 nm under a microspectrophotometer (Zeiss MPM800). The UV absorption spectra of the secondary wall and cell corner middle lamella were obtained for wavelengths of 250–350 nm using a 0.5-μm-wide measuring spot on the microspectrophotometer [18–20]. Measurements were taken at ten positions and averaged.

Tensile longitudinal modulus

Longitudinal tensile tests were performed as described by Kojima and Yamamoto [21]. The slices were attached to a handmade test machine and the test was conducted in a room maintained at 20 °C. To prevent slipping from the clamps, sandpaper was attached to the slice edges with quick-drying glue. Two spots 20 mm apart along the grain were marked on the tangential surface of the slices with a black graphite pencil to measure the displacement caused by the tensile load. A traveling microscope with an *xy*-microstage with 0.001 mm accuracy was used to measure the distance between the dots. The tensile elastic modulus of the slices (E^0) was calculated from the obtained stress–strain curve. The substantial elastic modulus of the cell wall (E^W) was defined as follows:

$$E^W = E^0 \frac{\rho^W}{\rho^0}, \quad (1)$$

where ρ^0 is the bulk density of the air-dried slice and ρ^W is the true density of the cell wall. After the tensile test, ρ^0 was determined by a gravimetric method and ρ^W was determined according to Whiting et al. [22]. A powdered slice was suspended in a separation liquid and vibrated. The separation liquid was a mixture of carbon tetrachloride and dioxane adjusted to a density of 1.30–1.50 g/mL. The density of the mixture in suspension after applying centrifugal force (10,000 rpm, 15 min) was the ρ^W of the slices [9].

Light microscopy and field-emission scanning electron microscopy

For the light microscopy observations, 1-μm-thick cross-sections were cut with a glass knife from the slices embedded in epoxy resin. The sections were stained with toluidine blue and examined using light microscopy. For the field-emission scanning electron microscopy (FE-SEM) observations, untreated slices were embedded in methacrylate resin and the cross-sectional surfaces were planed with a glass knife [23]. After removing the methacrylate resin in acetone, either polysaccharides or lignin were removed from the slices. Then the slices were dehydrated and freeze-dried with *t*-butanol. The dried slices were affixed to aluminum stubs, coated lightly with osmium and platinum-palladium, and examined using FE-SEM at an accelerating voltage of 1.5 kV and a 5-mm working distance.

Results and discussion

3D lignin slices after polysaccharide removal

Figure 1a shows an untreated tangential slice. Following periodate oxidation, the slice shrank markedly longitudinally (Fig. 1b). After polysaccharide removal, the slice was dark yellow and fragile (Fig. 1c).

After graded polysaccharide removal, wood slices were examined with light microscopy and FE-SEM (Fig. 1d–i). Figure 1d, g shows cross-sectional views of an untreated slice. Following periodate oxidation, the secondary wall thickness increased compared to an untreated slice (Fig. 1e). Periodate oxidation also caused the tracheid diameter to decrease. As shown in a micrograph taken at a higher FE-SEM magnification, the secondary wall and compound middle lamella were separated (Fig. 1h). As a result of polysaccharide removal, the secondary wall thickness decreased compared to a periodate-oxidized slice (Fig. 1f). In addition, the secondary wall was dented longitudinally compared to the compound middle lamella (Fig. 1i). This dent might have been caused by lignin shrinking in the secondary wall. Although slight changes occurred after polysaccharide removal, lignin slices retained the honeycomb structure (Fig. 1f) and the layered structure (Fig. 1i) of the cell walls. Therefore, we concluded that the 3D lignin slices were prepared successfully.

Figure 2a shows the changes in relative crystallinity with graded polysaccharide removal. The relative crystallinity of untreated slices was about 70 %. Following periodate oxidation subsequent to methylation, the relative crystallinity decreased substantially. During periodate oxidation, dialdehydes are formed on 1,2-diols in polysaccharides [10]. This dialdehyde structure might have

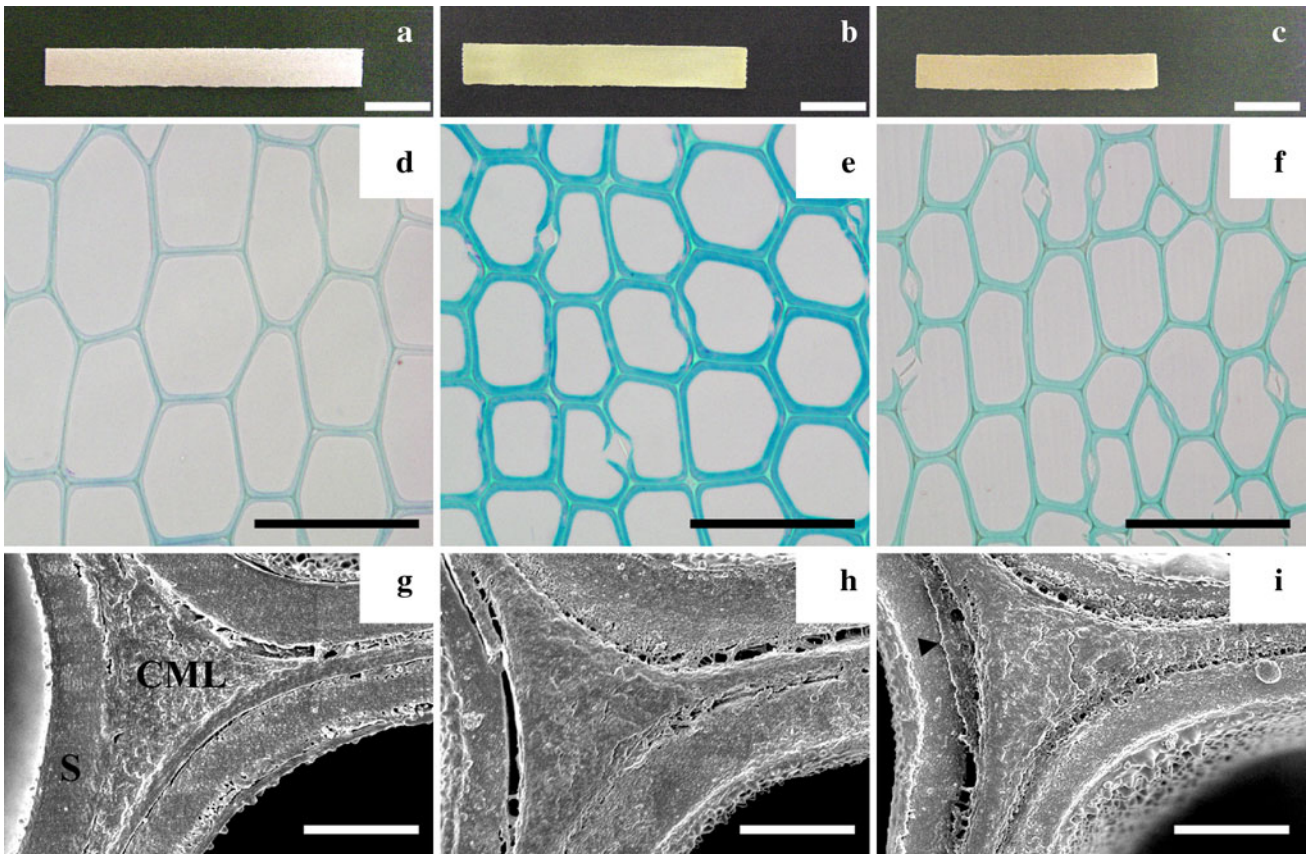

Fig. 1 Slices consisting of lignin with a 3D assembly in the cell walls. **1a–c** Tangential wood slices. **1d–f** Cross-sectional views of wood slices under light microscopy. **1g–i** The cell corner region taken at higher FE-SEM magnification. **a**, **d**, **g** Untreated slices. **b**, **e**, **h** Slices after periodate oxidation. **c**, **f**, **i** Slices after polysaccharide removal by repeating periodate oxidation and hydrolysis four times. *Bars:* 10 mm in **a-c**, 50 μm in **d-f**, 2 μm in **g-i**. *CML* compound middle lamella, *S* secondary wall. *Arrow heads* in **i** show that the secondary wall was dented longitudinally compared to the compound middle lamella

affected the cellulose microfibril crystalline structure. As a result of polysaccharide removal by repeating periodate oxidation and hydrolysis four times, the relative crystallinity decreased to only a small percentage.

Figure 2b shows the changes in oven-dried weight with graded polysaccharide removal. The weight of the wood slice increased slightly after periodate oxidation subsequent to methylation. As a result of polysaccharide removal with repeated periodate oxidation and hydrolysis, the final weight loss was about 54 %. Fukushima [24] reported that Sugi wood consists of about 70 % polysaccharides. After polysaccharide removal, some hemicellulose residue remained closely associated with lignin, having an essential role in the maintenance of cell wall assembly.

As a result of polysaccharide removal from untreated slices by repeated periodate oxidation and hydrolysis, the true density of the slices decreased from 1.42 to 1.37 g/cm^3, which was close to the density of lignin (1.340 g/cm^3) reported by Nishino and Norimoto [25]. Based on relative crystallinity, oven-dried weight, and true density, we concluded that the treatment removed the polysaccharides from the wood slices completely.

The E^w values of untreated slices with MFAs of 14°, 23°, 34°, and 42° were about 20, 15, 10, and 5 GPa, respectively. The standard deviation (SD) of E^w at a low MFA was high, while that at a high MFA was low as its contribution to the tensile load along the longitudinal axis of the cellulose microfibrils was small. The negative correlation between E^w and MFA is consistent with the trend reported by Yamamoto and Kojima [6].

Different results were observed after polysaccharide removal following periodate oxidation. Figure 2c shows the changes in the E^w with graded polysaccharide removal. Following periodate oxidation subsequent to methylation, the E^w decreased substantially. After periodate oxidation, the relative crystallinity decreased substantially, while slice weight remained nearly constant (dotted line in Fig. 2). The decrease in E^w was likely affected by the decrease in relative crystallinity. After complete polysaccharide removal by periodate oxidation and hydrolysis repeated four times, the E^w was 2.8 GPa, regardless of the MFA. The SD of the E^w decreased with graded polysaccharide removal. In general, microfibrils change their orientation angle by rotating stepwise, and alternate changes in the

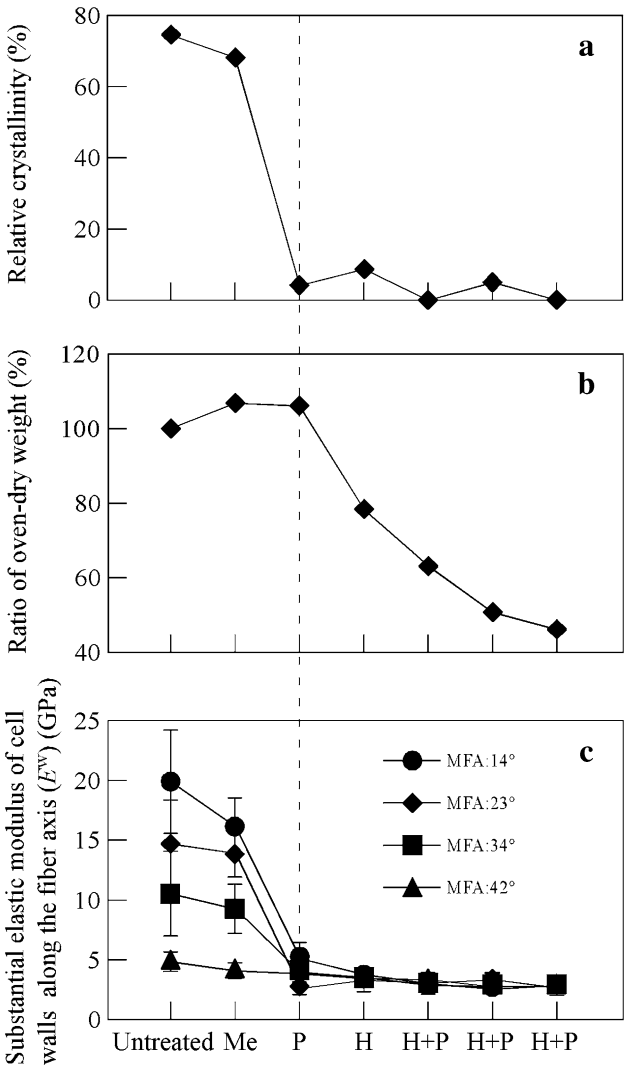

Fig. 2 Changes in the (**a**) relative crystallinity, (**b**) oven-dried weight ratio, and (**c**) substantial elastic modulus of cell walls (E^w). For graded polysaccharide removal, periodate oxidation and hydrolysis were repeated four times. The *dotted line* indicates the experimental values after periodate oxidation. *Me* methylation, *P* periodate oxidation, *H* hydrolysis

direction of rotation are repeated during the formation of thick layers in the walls [26, 27]. The cellulose microfibril orientation angle fluctuations could have affected the SD of the E^w. After polysaccharide removal, the SD of the E^w was likely low because of orientation angle fluctuations of the cellulose microfibril removal. From the microscopy results, the slices consisting of lignin retained their 3D assembly in the cell walls (Fig. 1d–i). Therefore, we concluded that the tensile elastic modulus of 3D lignin slices was 2.8 GPa at 10 % moisture content regardless of the MFA, similar to the 4 GPa for periodate lignin and 3 GPa for Klason lignin reported by Cousins [14]. It is interesting to note that elastic modulus of 3D lignin slices was not affected by the MFA while some researches pointed out that phenylpropane units in lignin are oriented in the direction of the cellulose microfibrils [11].

3D polysaccharide slices after lignin removal

Figure 3a shows an untreated tangential slice. Due to lignin removal, the slices were white (Fig. 3b, c). However, the slice size remained nearly constant.

After graded lignin removal, the wood slices were examined under light microscopy and FE-SEM (Fig. 3d–i). Figure 3d, g shows cross-sectional views of an untreated slice. Despite the 3-h lignin removal treatment, there were no significant changes in cell wall appearance (Fig. 3e, h). After the 6-h lignin removal treatment, the hexagonal shape of the cell walls had become slightly deformed (Fig. 3f). In addition, the secondary wall and compound middle lamella were partly separated. In images of the compound middle lamella taken under higher FE-SEM magnification, it could be seen that most of the lignin was removed (Fig. 3i). Although slight changes occurred after lignin removal, polysaccharide slices retained the honeycomb structure (Fig. 3f) and the layered structure (Fig. 3i) of the cell walls. Therefore, we considered that the 3D polysaccharide slices were prepared successfully.

Figure 4a shows the changes in UV absorbance with graded lignin removal. For the untreated slices, the UV absorbance of the secondary wall and cell corner middle lamella was about 0.5 and 0.8, respectively. After the 6-h lignin removal treatment, both values decreased to about 0.05. Figure 4b shows the change in oven-dried weight with graded lignin removal. As a result of the 6-h lignin removal treatment, the final weight loss was about 28 %, which was similar to the amount of lignin in Sugi wood, 31.4 %, reported by Fukushima [24].

Figure 4c shows the changes in relative crystallinity with graded lignin removal. The relative crystallinity remained almost constant throughout the treatment. Therefore, we concluded that the polysaccharide remained in the cell wall after lignin removal.

After lignin removal, the true density of the slices increased from 1.42 to 1.49 g/cm^3. Nishino and Norimoto [25] reported that the density of crystalline and non-crystalline cellulose was 1.592 and 1.469 g/cm^3, respectively. The 1.49 g/cm^3 of 3D polysaccharide slices is likely an accurate value of the true density of the polysaccharides in Sugi wood cell walls. Based on UV absorbance, oven-dried weight, and true density, we concluded that the lignin was removed completely from the wood slices.

Figure 4d shows the change in E^w with graded lignin removal. The E^w values of 3D polysaccharide slices were negatively correlated with MFA. The E^w in each slice remained almost constant throughout the treatment regardless of MFA. The SD of E^w also remained high,

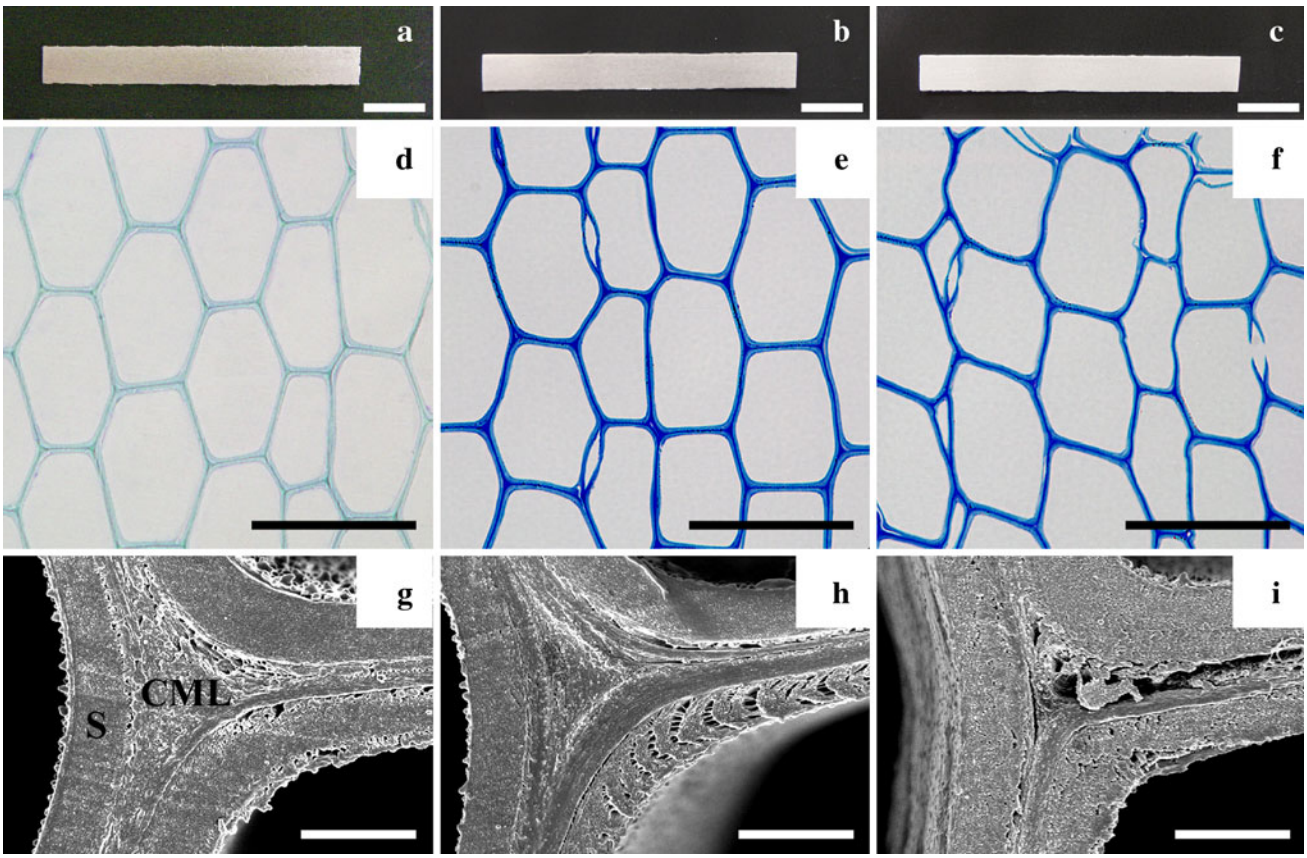

Fig. 3 Slices consisting of polysaccharide with a 3D assembly in the cell walls. **3a–c** Tangential wood slices. **3d–f** Cross-sectional views of wood slices under light microscopy. **3g–i** The cell corner region taken at higher FE-SEM magnification. **a**, **d**, **g** Untreated slices. **b**, **e**, **h** Slices after lignin removal treatment for 3 h. **c**, **f**, **i** Slices after the 6-h lignin removal treatment. *Bars:* 10 mm in **a-c**, 50 μm in **d-f**, 2 μm in **g-i**. *CML* compound middle lamella, *S* secondary wall

possibly due to orientation angle fluctuations of the cellulose microfibrils remaining in the cell walls. The SD of E^w with high MFAs was relatively low, as its contribution to the tensile load along the longitudinal axis of the cellulose microfibrils was small. Based on these results, we concluded that cellulose microfibrils governed E^w and controlled the mechanical anisotropy.

3D intertwining of wood polymers and mechanical properties of the wood cell wall

Despite the fact that cellulose content increased after lignin removal, values of E^w slightly decreased regardless of MFA (Fig. 4d). From the microscopy results, the slice consisting of polysaccharide retained its 3D assembly in the cell wall (Fig. 3d–i). Furthermore, the relative crystallinity remained constant throughout the treatment (Fig. 4c).

There are two possible reasons why E^w did not become higher after lignin removal. First, lignin removal caused an artifactual deterioration in the polysaccharide slices at the level of macromolecular aggregate, such as micro-voids, disaggregation, or delamination among cellulose microfibrils, and so forth. Second, rigid and fusiform-shaped cellulose crystallites are dispersed in the soft matrix of amorphous polysaccharide, and those crystallites are loosely connected to each other by the intermediary of those polysaccharide, e.g., hemicellulose and non-crystalline cellulose. Those suggest that the rigid cellulose crystallite can optimize its strong mechanical performance in the polysaccharide framework of the wood cell wall in combination with the ligninification.

Conclusion

We prepared 3D lignin and 3D polysaccharide slices and measured their tensile elastic moduli to investigate the mechanical properties of the individual component polymers with a 3D assembly mode in the cell walls.

The elastic modulus of the 3D lignin slices was 2.8 GPa, regardless of the microfibril angle (MFA) in the slices. This shows that the lignin behaves as an isotropic matrix in the wood cell wall. The elastic moduli of the 3D

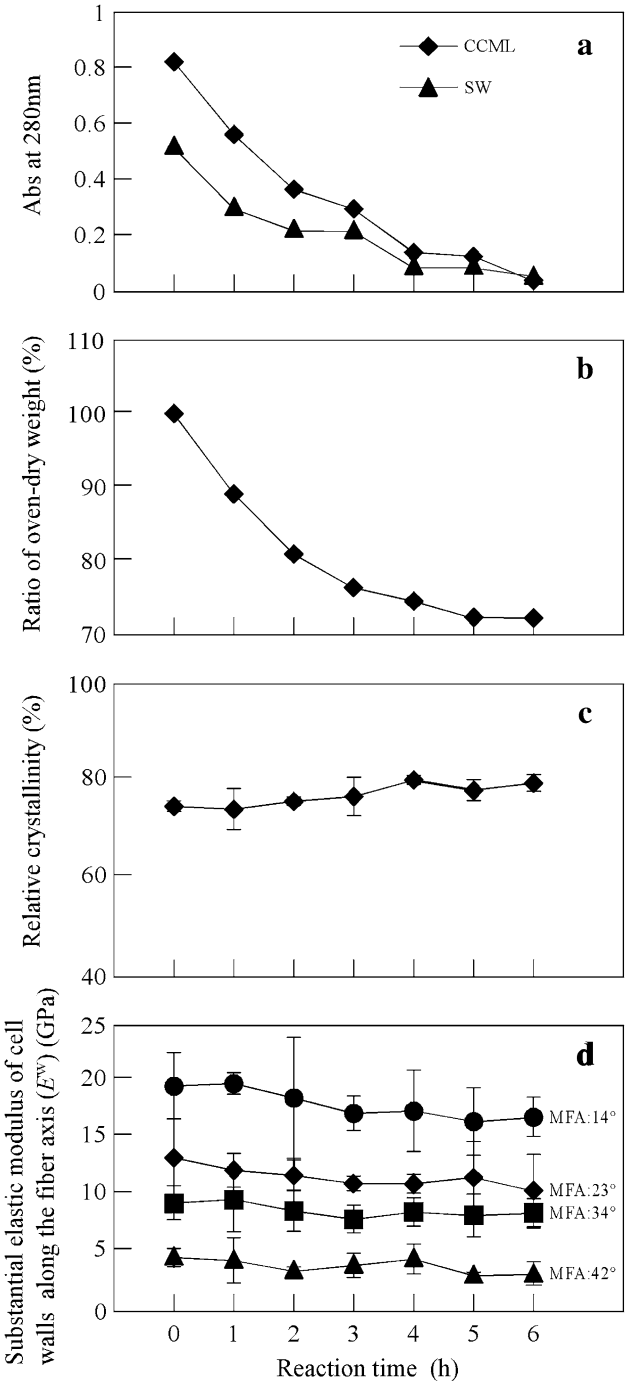

Fig. 4 Changes in the (**a**) UV absorbance of the secondary wall (*SW*) and cell corner middle lamella (*CCML*), (**b**) oven-dried weight ratio, (**c**) relative crystallinity, and (**d**) substantial elastic modulus of the cell wall (E^w). The graded lignin removal treatment was conducted for 6 h

polysaccharide slices with MFAs of 14°, 23°, 34°, and 42° became 18, 12, 9, and 4 GPa, respectively. This shows that the rigid cellulose microfibrils are oriented in a certain direction in the polysaccharide, thus governs the mechanical performance of the wood cell wall.

However, E^w slightly decreased after lignin removal despite the fact that cellulose content increased. This is because rigid cellulose crystallites are dispersed in the 3D polysaccharide, which are loosely connected to each other by the intermediary of non-crystalline substances, e.g., hemicellulose and non-crystalline cellulose. In addition, artifactual deterioration was caused in the polysaccharide slices at the level of macromolecular aggregate by lignin removal. Those suggest that the rigid cellulose crystallite exerts its strong performance in the polysaccharide framework of the wood cell wall in combination with the ligninification.

Acknowledgments We greatly appreciated cooperation of Mr. Yasuji Imaizumi, Mr. Naoki Takabe, and Mr. Norio Yamaguchi from the Nagoya University Experimental Forest for their assistance in logging the sample trees.

References

1. Cave ID (1972) Swelling of a fiber reinforced composite in which the matrix is water reactive. Wood Sci Technol 6:157–161
2. Yamamoto H, Alméras T (2007) Mathematical verification of the reinforced-matrix hypothesis by Mori-Tanaka theory. J Wood Sci 53:505–509
3. Mark RE (1967) Cell wall mechanics of tracheids. University Press, New York, pp 27–58
4. Page DH, El–Hosseiny F, Winkler K, Lancaster APS (1977) Elastic modulus of single wood pulp fibers. Tappi 60:114–117
5. Sobue N, Asano I (1976) Studies on the fine structure and mechanical properties of wood. Mokuzai Gakkaishi 22:211–216
6. Yamamoto H, Kojima Y (2002) Properties of the cell wall constituents in relation to the longitudinal elasticity of wood: part 1. Formulation of the longitudinal elasticity of an isolated wood fiber. Wood Sci Technol 36:55–74
7. Terashima N (1990) A new mechanism for formation of a structurally ordered protolignin macromolecule in the cell wall of tree xylem. J Pulp Pap Sci 16:J150–J155
8. Salmen L, Olsson AM (1998) Interaction between hemicellulose, lignin and cellulose: structure-property relationships. J Pulp Pap Sci 24:99–103
9. Terashima N, Kitano K, Kojima M, Yoshida M, Yamamoto H, Westermark U (2009) Nanostructural assembly of cellulose, hemicellulose, and lignin in the middle layer of secondary wall of ginkgo tracheid. J Wood Sci 55:409–416
10. Terashima N, Yoshida M (2006) Ultrastructure of lignified plant cell wall observed by field-emission scanning electron microscopy: observations on periodate lignin prepared from *Ginkgo biloba*. Cellul Chem Technol 40:727–733
11. Akerholm M, Salmen L (2003) The mechanical role of lignin in the cell wall of spruce tracheids. Holzforschung 57:459–465
12. Sakurada I, Nukushina A, Ito T (1962) Experimental determination of the elastic modulus of crystalline regions in oriented polymers. J Polym Sci 57:651–660
13. Nishino T, Takano K, Nakamae K (1995) Elastic modulus of the crystalline regions of cellulose polymorphs. J Polym Sci B Polym Phys 33:1647–1651
14. Cousins WJ (1976) Elastic modulus of lignin as related to moisture content. Wood Sci Technol 10:9–17
15. Maekawa E, Koshijima T (1983) Evaluation of the acid chlorite method for the determination of wood holocellulose. Mouzai Gakkaishi 29:702–707

16. Yamamoto H, Okuyama T, Yoshida M (1993) Method of determining the mean microfibril angle of wood over a wide range by the improved Cave's method. Mokuzai Gakkaishi 39:375–381
17. Alexander LE (1969) X-ray diffraction methods in polymer science. Wiley, New York
18. Okuyama T, Takeda H, Yamamoto H, Yoshida M (1998) Relation between growth stress and lignin concentration in the cell wall: ultraviolet microscopic spectral analysis. J Wood Sci 44:83–89
19. Yoshida M, Ohta H, Okuyama T (2002) Tensile growth stress and lignin distribution in the cell walls of black locust (*Robinia pseudoacacia*). J Wood Sci 48:99–105
20. Yoshida M, Ohta H, Yamamoto H, Okuyama T (2002) Tensile growth stress and lignin distribution in the cell walls of yellow poplar, *Liriodendron tulipifera* Linn. Trees 16:457–464
21. Kojima Y, Yamamoto H (2004) Properties of the cell wall constituents in relation to the longitudinal elasticity of wood: part 2. Origin of the moisture dependency of the longitudinal elasticity of wood. Wood Sci Technol 37:427–434
22. Whiting P, Favis BD, St-Germain FGT, Goring DAI (1981) Fractional separation of middle lamella and secondary wall tissue from spruce wood. J Wood Chem Technol 1:29–42
23. Sano Y (2004) Intervascular pitting across the annual ring boundary in *Betula platyphylla* var. *japonica* and *Fraxinus mandshurica* var. *japonica*. IAWA J 25:129–140
24. Fukushima K (2010) Mokuzai no Sosei. In: Meshitsuka G (ed) Mokushitsu no Kagaku (in Japanese). Bun'eido, Tokyo, pp 3–4
25. Nishino Y, Norimoto M (1990) Structure and Anisotropy of Dielectric Constant in Hardwood (in Japanese). Wood Res Tech Notes 26:78–90
26. Kataoka Y, Saiki H, Fujita M (1992) Arrangement and superimposition of cellulose microfibrils in the secondary walls of coniferous tracheids. Mokuzai Gakkaishi 38:327–335
27. Abe H, Funada R (2005) Review—the orientation of cellulose microfibrils in the cell walls of tracheids in conifers: a model based on observations by field emission scanning electron microscopy. IAWA J 26:161–174